Single-electron tunneling into randomly distributed double-electron states: Linear voltage and temperature dependences of the conductance of high-T_c tunnel junctions

M. Hurd, R. I. Shekhter,* and G. Wendin
Institute of Theoretical Physics, Chalmers University of Technology, S-412 96 Göteborg, Sweden
(Received 30 April 1992)

In sandwich-type tunnel junctions of high-T_c materials the conductance is observed to have a large zero-bias value, linear voltage dependence at low temperature, and linear temperature dependence at low voltage. We suggest a model of single-electron tunneling into randomly distributed (disordered) local centers with strong interelectron attraction to explain these features. In point-contact tunnel junctions these features should be absent due to local homogeneity in contacts of small area. We compare predictions of the model with experiment.

I. INTRODUCTION

Tunneling measurements, which are extremely useful in investigations of conventional superconductors, do not have any straightforward interpretation in the case of high-T_c compounds. Analyzing all experimental results one can, however, single out a common tendency. The conductance $G=dI/dV$ obtained for point-contact tunneling structures and those obtained for usual sandwich-type tunneling junctions are qualitatively different.[1] These distinctions mainly show up in (i) the tunneling conductance $G(V,T)$ at voltage $V=0$ and temperature $T=T_c$, and (ii) the type of voltage dependence of G over a large bias range ($V\sim 50-100$ mV). Experiments recently carried out on sandwich-type contacts of large area (0.1×0.1 mm^2) demonstrate quite reproducible results:[2-8] (i) large values of $G(0,0)/G_N\sim 0.1-0.5$, $G_N=G(0,T_c)$ is the normal-state conductance; (ii) linear voltage dependence of the background in $G(V,T)$ in the range of large voltages up to 50–200 mV. In contrast, the data obtained for the best point contacts have the following features: (i) small values of $G(0,0)/G_N \lesssim 0.01$;[9-15] (ii) either the voltage dependence of the background is absent,[9-11] or is it nonregular and asymmetric with respect to bias sign.[12-15] The most evident example of the qualitative distinction between point- and sandwich-type contacts obtained for the 80K phase of the Bi-Sr-Ca-Cu-O system, investigated in Refs. 2 and 10, is shown in Fig. 1. It should also be mentioned that the results for point contacts of comparitatively large area (250×250 μm^2) are close to those obtained for sandwich junctions.[16]

Existing theoretical models which predict a linear-voltage dependence of tunneling conductance appeal either to intrinsic properties of high-T_c materials [tunneling into the resonating-valence-bond (RVB) state,[17-19] inelastic tunneling with generation of paramagnons,[20-21] tunneling of quasibosonic electron pairs[22] and bipolarons[23]] or to properties of the tunneling barrier itself (field effect in electron tunneling[1,24]). Such approaches do not explain why the I-V curves are different for different types of tunnel junctions.

Surface-layer investigations of high-T_c materials by means of scanning tunneling microscopy (STM) (Refs. 10 and 25) demonstrate directly a substantial inhomogeneity of the scale 1000–1500 Å,[10] where superconducting parts as well as dielectric and metallic regions coexist.[25] In the tunnel point contacts, the size of the area involved in tunneling is usually about 100–1000 Å,[13] and at most a minor set of inhomogeneities is probed, leading to discrete and irregular structures in $G(V)$ curves, while for sandwich-type junctions, with area of 0.1×0.1 mm^2, the tunneling is determined by currents averaged on a wide range of surface inhomogeneities.

It is obvious, due to substantial proportion of nonsuperconducting surface regions in large-area contacts, that tunneling into the superconductor, which in the completely homogeneous case is blocked because of the superconducting gap, would be allowed. Owing to this fact large values of tunneling conductance $G(0,0)$ may be explained.

Within the theory of local pairing[22,26-29] we would like to formulate a model of single-electron tunneling which enables us to explain *the relation between the linear background conductance and the surface disorder.* The main features in this model are the following:

(a) Presence in high-T_c material of localized electronic states (local centers, LC) along with conventional band electrons; hybridization between the two types of electrons is also supposed to exist;

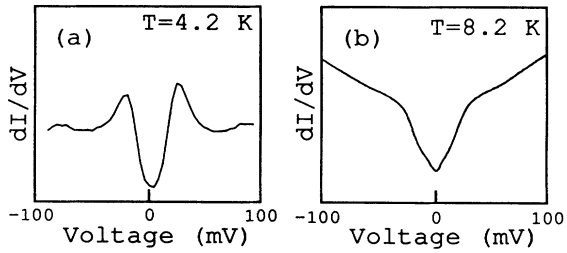

FIG. 1. Conductance (dI/dV) vs voltage for the 80K phase of the Bi-Sr-Ca-Cu-O system is shown for (a) a point-contact tunneling junction (from Ref. 10) and (b) a sandwich-type tunneling junction (from Ref. 2). The units for conductance are arbitrary in both figures.

(b) strong electron-electron attraction within LC (negative-U centers) causing the electrons to order in pairs, so-called local pairs;

(c) distribution of LC energies as a result of surface inhomogeneities.

Items (a) and (b) represent the idea of local pairing. Investigations of models based on (a) and (b) have been presented in a number of works,[22,26–29] and one of the objects of these investigations has been to relate the local pair concept to high-T_c superconductivity. Here our prime interest is the normal-state properties of high-T_c materials and to test if it is possible to explain the much discussed results of different kinds of tunneling spectroscopies within a model of local pairing. The main theme of this paper is the difference between measurements of small-area and large-area tunneling junctions.

II. THE MODEL

The Hamiltonian of the tunneling structure, shown for instance in Fig. 2(a), has the form

$$H = H_M + H_C + H_T + eV \sum_{\mathbf{k}\sigma} b^\dagger_{\mathbf{k}\sigma} b_{\mathbf{k}\sigma} \ , \tag{1}$$

where H_M and H_C are the Hamiltonians for the normal and the strongly correlated metal, respectively, and H_T is the tunneling Hamiltonian. V is the voltage across the junction.

The normal metal (M) is described by the Hamiltonian

$$H_M = \sum_{\mathbf{k}\sigma} \varepsilon^b_{\mathbf{k}} b^\dagger_{\mathbf{k}\sigma} b_{\mathbf{k}\sigma} \ . \tag{2}$$

All energies are measured with respect to the chemical potential at $T=0$.

The system we are interested in corresponds to H_C and is described by a model of local pairing (correlated metal, CM). The starting point is then a periodically extended Anderson model:[22,29]

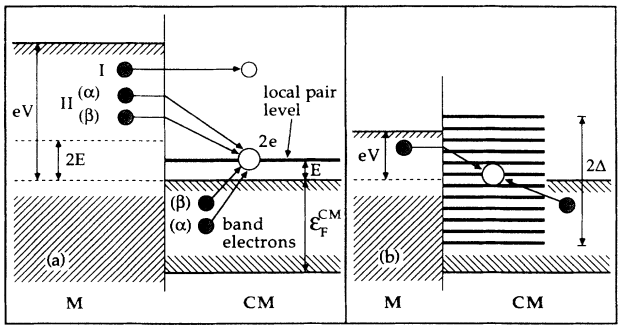

FIG. 2. (a) Diagrams of electron tunneling from the conventional metal (M) to the strongly correlated metal (CM). Process I shows tunneling from the band in M to the band in CM. Processes II (a) and (b) show different channels of tunneling from the band in M to a local center in CM accompanied by the transition from the band in CM to the same local center. $2E$ is the local pair energy relative to the chemical potential and is also the threshold energy for processes II. (b) The local pair levels are distributed in an interval of 2Δ. The case when $eV<\Delta$ is shown.

$$H_C = \sum_{\mathbf{k}\sigma} \varepsilon^a_{\mathbf{k}} a^\dagger_{\mathbf{k}\sigma} a_{\mathbf{k}\sigma} + E_1 \sum_{j\sigma} c^\dagger_{j\sigma} c_{j\sigma} + U \sum_j c^\dagger_{j\sigma} c_{j\sigma} c^\dagger_{j\bar{\sigma}} c_{j\bar{\sigma}} + \frac{1}{\sqrt{N_a}} \sum_{\mathbf{k}j\sigma} (t_{\mathbf{k}} e^{-i\mathbf{k}\cdot\mathbf{R}_j} a_{\mathbf{k}\sigma} c^\dagger_{j\sigma} + \text{H.c.}) \ . \tag{3}$$

In the Hamiltonian above there are two electronic subsystems. The subsystem represented by the a operators consists of wide-band electrons characterized by a Bloch momentum $\mathbf{k}$, and the other subsystem, represented by the c operators, consists of localized states characterized by a site label j. The first and second terms are the energy of the electrons in the wide band and the energy of singly occupied sites, respectively. The localized states on the same site (with opposite spins) interact with each other by the Hubbard energy U. Considering local pairs this energy is negative and assumed to be large in magnitude. The last term is the hybridization between the two subsystems, and in the analysis which follows this term is treated as small compared to the other terms in H_C. In the situation discussed above with large negative Hubbard energy and small hybridization, the subsystem of localized states prefers to order in empty and doubly occupied sites. The natural units, so to speak, of the subsystem are then not the c operators but rather two-particle operators that more efficiently describe the situation on each site. The slave boson representation[30,31] is often used in this context. Here we use it only for technical reasons because of its notational ability. The localized states of CM on each site j are represented by two Fermi operators, $s_{j\sigma}$, one for spin up and one for spin down, and also two Bose operators, e_j and d_j. One defines $s_{j\sigma}$, e_j, and d_j to annihilate a singly occupied state with spin projection σ, an empty state, and a doubly occupied state on the site j, respectively. These operators are not independent but fulfill the constraint $e^\dagger_j e_j + \sum_\sigma s^\dagger_{j\sigma} s_{j\sigma} + d^\dagger_j d_j = 1$, and the electron operator is rewritten like $c^\dagger_{j\sigma} = s^\dagger_{j\sigma} e_j + \text{sgn}(\sigma) d^\dagger_j s_{j\bar{\sigma}}$. Using these operators we reformulate Eq. (3):

$$H_C = \sum_{\mathbf{k}\sigma} \varepsilon^a_{\mathbf{k}} a^\dagger_{\mathbf{k}\sigma} a_{\mathbf{k}\sigma} + E_1 \sum_{j\sigma} s^\dagger_{j\sigma} s_{j\sigma} + E_2 \sum_j d^\dagger_j d_j + \frac{1}{\sqrt{N_a}} \sum_{\mathbf{k}j\sigma} \{ t_{\mathbf{k}} e^{-i\mathbf{k}\cdot\mathbf{R}_j} a_{\mathbf{k}\sigma} [s^\dagger_{j\sigma} e_j + \text{sgn}(\sigma) d^\dagger_j s_{j\bar{\sigma}}] + \text{H.c.} \} \ ,$$
$$E_2 = 2E_1 + U \ . \tag{4}$$

In the tunneling Hamiltonian H_T we have two tunneling channels, either band-to-band or band-to-LC levels [see Fig. 2(a)]:

$$H_T = \sum_{\mathbf{kp}} t^a_{\mathbf{kp}} b_{\mathbf{k}\sigma} a^\dagger_{\mathbf{p}\sigma} + \frac{1}{\sqrt{N_b}} \sum_{\mathbf{k}j\sigma} t^c_{\mathbf{k}j} b_{\mathbf{k}\sigma} [s^\dagger_{j\sigma} e_j + \text{sgn}(\sigma) d^\dagger_j s_{j\bar{\sigma}}] + \text{H.c.} \tag{5}$$

III. CALCULATION OF THE CONDUCTANCE

We now calculate the tunneling current by using the standard method of expansion in the small tunneling Hamiltonian. Taking into account only single-electron tunneling, we keep only the lowest-order contribution in such an expansion. First we define the following quantities:

$$P=\sum_{\mathbf{kp}} t^a_{\mathbf{kp}} b_{\mathbf{k}\sigma} a^\dagger_{\mathbf{p}\sigma} ,$$
$$Q=\frac{1}{\sqrt{N_b}}\sum_{\mathbf{k}j\sigma} t^c_{\mathbf{k}j} b_{\mathbf{k}\sigma}[s^\dagger_{j\sigma} e_j+\mathrm{sgn}(\sigma) d^\dagger_j s_{j\bar{\sigma}}] , \tag{6}$$

and their time dependence

$$P(t)=e^{i(H_N+H_C)t/\hbar} P e^{-i(H_N+H_C)t/\hbar} ,$$
$$Q(t)=e^{i(H_N+H_C)t/\hbar} Q e^{-i(H_N+H_C)t/\hbar} . \tag{7}$$

Then the current is given by

$$I=\frac{2e}{\hbar^2}\mathrm{Re}\int_{-\infty}^{t} dt' e^{ieV(t-t')/\hbar} \times\langle[P(t)+Q(t),P^\dagger(t')+Q^\dagger(t')]\rangle , \tag{8}$$

where the $\langle\ \rangle$ brackets denote the thermal average. We make an expansion in hybridization by using the canonical transformation due to Schrieffer and Wolff.[32] This means we change any operator X into a new operator by the rule

$$X\rightarrow e^S X e^{-S} , \tag{9}$$

and choose S to have the form

$$S=\frac{1}{\sqrt{N_a}}\sum_{\mathbf{k}j\sigma} e^{-i\mathbf{k}\cdot\mathbf{R}_j} a_{\mathbf{k}\sigma} \times\{S_1(\mathbf{k}) s^\dagger_{j\sigma} e_j+S_2(\mathbf{k})\,\mathrm{sgn}(\sigma) d^\dagger_j s_{j\bar{\sigma}}\} -\mathrm{H.c.} , \tag{10}$$

where $S_1(\mathbf{k})=t_{\mathbf{k}}/(E_1-\varepsilon^a_{\mathbf{k}})$ and $S_2(\mathbf{k})=t_{\mathbf{k}}/(E_2-E_1-\varepsilon^a_{\mathbf{k}})$ are the hybridization amplitudes. According to Eq. (4), H_C is a sum of H_0 and V, where V corresponds to the last term in Eq. (4). After the transformation H_C is changed in the following way:

$$H_C\rightarrow H_0+V'+\cdots,\quad V'=\tfrac{1}{2}[S,V] , \tag{11}$$

where V' is second order in hybridization and further terms are of higher order. The first-order term in V has been removed by the special choice of S, Eq. (10). Writing down the current we have three types of contributions: (i) corrections from the statistical operator; (ii) terms from the exponentials in the time dependence of Eq. (7); (iii) terms from the expansion of the exponentials $e^S P e^{-S}$ and $e^S Q e^{-S}$ appearing in Eq. (8). Considering (i) and (ii), we can formally write

$$e^{\beta H_0} e^{-\beta(H_0+V')}=1-\int_0^\beta d\tau e^{H_0\tau} V' e^{-H_0\tau}+\cdots , \tag{12a}$$
$$e^{iH_0 t/\hbar} e^{-i(H_0+V')t/\hbar}=1-\frac{i}{\hbar}\int_0^t dt' e^{iH_0 t'/\hbar} V' e^{-iH_0 t'/\hbar} +\cdots . \tag{12b}$$

To calculate the current to zeroth and first order in hybridization we are not interested in the corrections of Eq. (12) since these are now second order in hybridization. However, from (iii) we find first-order terms. Below we list them together with the zeroth-order terms:

$$I_0=\frac{2e}{h}\left[\sum_{\mathbf{kp}}|t^a_{\mathbf{kp}}|^2\delta(\varepsilon^a_{\mathbf{p}}-\varepsilon^b_{\mathbf{k}}-eV)[n(\varepsilon^b_{\mathbf{k}})-n(\varepsilon^a_{\mathbf{p}})]+\sum_{\mathbf{k}j}|t^c_{\mathbf{k}j}|^2(\delta(E_1-\varepsilon^b_{\mathbf{k}}-eV)\{n(\varepsilon^b_{\mathbf{k}})n_{jh}-n_{j\sigma}[1-n(\varepsilon^b_{\mathbf{k}})]\} +\delta(E_2-E_1-\varepsilon^b_{\mathbf{k}}-eV)\{n(\varepsilon^b_{\mathbf{k}})n_{j\bar{\sigma}}-[1-n(\varepsilon^b_{\mathbf{k}})]n_{jd}\})\right] , \tag{13}$$

$$I_1=\frac{4e}{h}\frac{1}{\sqrt{N_a}}\sum_{\mathbf{kp}j} t^a_{\mathbf{kp}}(t^c_{\mathbf{k}j})^* e^{-i\mathbf{p}\cdot\mathbf{R}_j}(\delta(\varepsilon^a_{\mathbf{p}}-\varepsilon^b_{\mathbf{k}}-eV)[S_1(\mathbf{p})(n_{jh}+n_{j\sigma})+S_2(\mathbf{p})(n_{j\bar{\sigma}}+n_{jd})][n(\varepsilon^b_{\mathbf{k}})-n(\varepsilon^a_{\mathbf{p}})] +\delta(E_1-\varepsilon^b_{\mathbf{k}}-eV)S_1(\mathbf{p})\{n_{j\sigma}[1-n(\varepsilon^b_{\mathbf{k}})]-n(\varepsilon^b_{\mathbf{k}})n_{jh}\} +\delta(E_2-E_1-\varepsilon^b_{\mathbf{k}}-eV)S_2(\mathbf{p})\{[1-n(\varepsilon^b_{\mathbf{k}})]n_{jd}-n(\varepsilon^b_{\mathbf{k}})n_{j\bar{\sigma}}\}) . \tag{14}$$

Here $n(\varepsilon)$ is the Fermi function for the band electrons in M and CM. The functions $n_{jh}=1/Z_j$, $n_{j\sigma}=\exp(-\beta E_1)/Z_j$, and $n_{jd}=\exp(-\beta E_2)/Z_j$, where

$$Z_j=1+2\exp(-\beta E_1)+\exp(-\beta E_2)$$

and $\beta=(k_B T)^{-1}$, are the distribution functions for zero, single, and double occupancy on the site j.

In Eq. (13) we recognize the standard band-to-band tunneling described by $|t^a_{\mathbf{kp}}|^2$ and the band-to-LC tunneling described by $|t^c_{\mathbf{k}j}|^2$. According to the theory of local pairing,[22] superconductivity is most favorable (highest T_c) when the local pairs are close to the Fermi energy. This means that $E_2\approx 0$, and this is then the case of interest regardless of our investigation being made in the normal state. Also, since the expansion above assumes $-U$ being large, E_1 and $E_2-E_1\approx -E_1$ are far above and far below the Fermi energy, respectively. $n_{j\sigma}$ is then turned off to zero, and the band-to-LC transitions in the second sum of Eq. (13) are not allowed because we study only the small-voltage regime, where the restriction

$|eV| < E_1$ is clearly satisfied. I_1 does not show any new characteristic features compared to I_0, but is just a renormalization of the simple processes responsible for I_0. The voltage dependence of the conductance $G = dI/dV$ is the same for both G_0 and G_1. When we write down G_0, the standard approximations are made: $|t^a_{\mathbf{kp}}|^2 = |t^a|^2$ is independent of momenta and the electronic density of states is independent of energy, justified by the small-voltage limit. As a result,

$$G_0 = (2e^2/h) N_F^a N_F^b |t^a|^2 . \tag{15}$$

This expression, independent of temperature, is valid when $k_B T$ is much smaller than the Fermi energies of the a and b band, which usually is the case. N_F^a and N_F^b are the electronic density of states at the Fermi energy for the a states and the b states, respectively. The conductance G_0, and G_1 as well, has no voltage dependence.

Before introducing corrections of second order in hybridization we want to make contact with a physical picture of this tunneling problem. In Fig. 2 the diagrams of electron tunneling from the ordinary metal (M) to the metal with strong electron correlations (correlated metal, CM) are presented. Figure 2(a) illustrates different possibilities for single-electron tunneling. Besides conventional band-to-band electron tunneling [see arrow I in Fig. 2(a)], there is also electron tunneling between the band in M and the LC states in CM. At sufficiently low voltage ($eV < E - U/2 = E_1$, $U < 0$ is the Hubbard energy, and $2E = E_2$ the local pair energy), the simple tunneling process of taking one electron from the M side into an empty LC state (on the CM side) is energetically forbidden. Only tunneling processes resulting in the appearance of two electrons in LC are possible. Even if we restrict ourselves to single-electron tunneling, it is possible to get such a double occupation of LC by *inelastic tunneling*, combining single-electron tunneling into LC with transitions from the wide band in CM into the same LC due to hybridization [see Fig. 2(a), paths II]. It is very important to stress that there is a number of different channels for such a complex transition corresponding to the same final energy of a double-electron state on LC, e.g., (α) and (β) in Fig. 2(a). Because of the necessity to have two initial band electrons in both metals with a given total energy to form a bonding state, the tunneling into LC is possible only at sufficiently large voltages $eV > 2E$, where $2E$ is twice the distance between LC energy and chemical potential [see Fig. 2(a)]. This means that we should have a threshold for single-electron tunneling into LC and, correspondingly, a steplike voltage dependence of the tunnel conductance. In a homogeneous material LC energies should be the same all over the bulk, as in Fig. 2(a). This homogeneity is not present at the surface of high-T_c materials, as mentioned above, but rather the surface is divided into different regions of local homogeneity. Each such region is then associated with a certain LC energy and a steplike conductance with threshold voltage twice this LC energy. Point contacts only probe one or a few of these regions, leading to a superposition of steplike conductances associated with each of these regions. Having larger contact area and approaching the limit of sandwich junctions, a large number of locally homogeneous regions are probed, and a large number of randomly distributed threshold energies should be present to smooth out the conductance. The tunneling diagram for this case is shown in Fig. 2(b). Such an averaging results in a linear voltage dependence of the normal-state conductance.

Investigating the second-order contribution of the expansion we want to find the term(s) corresponding to the processes denoted by II in Fig. 2(a). The first-order corrections of Eq. (12) only enter as Hartree-like potential contributions in correlation functions such as $\langle a_{k\sigma}(t') a^\dagger_{k\sigma}(t) \rangle$ and $\langle c_{i\sigma}(t') c^\dagger_{j\sigma}(t) \rangle$, appearing in Eq. (8). Summing all these Hartree-like terms, the energy levels are shifted due to the interaction between the two electronic subsystems. This shift is of the order of the interaction energy, which is considered to be small. Except from renormalization of the tunneling matrix element the results are not different from Eq. (15).

The term of interest we find by calculating the large number of terms emerging from the expansion of $e^S P e^{-S}$ and $e^S Q e^{-S}$ appearing in Eq. (8). Inspecting the arguments of the δ functions associated with each of these terms, we find one term to be special and it obviously corresponds to processes II of Fig. 2(a). The other terms are of the same kind as those of I_0 and I_1. We name the special term I_2:

$$\begin{aligned} I_2 = \frac{2e}{h} \frac{1}{N_a N_b} \sum_{\mathbf{k}pj} |t^c_{\mathbf{k}j}|^2 |S_1(\mathbf{p}) - S_2(\mathbf{p})|^2 \\ \times \delta(E_2 - \varepsilon^a_{\mathbf{p}} - \varepsilon^b_{\mathbf{k}} - eV) \\ \times \{ n_{jh} n(\varepsilon^a_{\mathbf{p}}) n(\varepsilon^b_{\mathbf{k}}) - n_{jd} [1 - n(\varepsilon^a_{\mathbf{p}})] \\ \times [1 - n(\varepsilon^b_{\mathbf{k}})] \} . \end{aligned} \tag{16}$$

We now investigate the conductance $G(V,T) = G_0 + G_2(V,T)$, where $G_2 = dI_2/dV$, in the zero-temperature limit. To simplify, and to stress the important features of G_2, we assume that all the LC energies are concentrated in the energy interval 2Δ, which is smaller than the Fermi energy of the a band, according to some distribution function. In this case, at voltages $V \leq \Delta/e$ we can neglect momentum dependences of $t^{a,c}$ and $S_{1,2}$ and use electronic density of states independent of energies. We also neglect site dependence of t^c. Then we rewrite the sum $\sum_j$ in Eq. (16) as an integral $\int dE\, F(E)$, where $F(E)$ is the distribution function for LC levels involved in tunneling. For zero temperature we have from Eq. (16)

$$\begin{aligned} G_2(V, T=0) = \frac{2e^2}{h} \frac{N'}{N_a N_b} N_F^a N_F^b \langle |t^c|^2 |S_1 - S_2|^2 \rangle_{\text{average}} \\ \times \int dE\, F(E) \{ \theta(-E) \theta(2E - eV) \\ + \theta(E) \theta(-2E + eV) \} . \end{aligned} \tag{17}$$

N' is the number of local levels involved in tunneling, and $\langle \cdots \rangle_{\text{average}}$ denotes the average over momentum orientation for $\mathbf{k}$ and $\mathbf{p}$ on the Fermi surfaces and over the po-

sitions for the local levels j. Notice that G_2 is proportional to N' or, in other words, the junction area, and does not depend on the volume of the system, since $N_F^a N_F^b/(N_a N_b)$ is independent of the volume.

IV. RESULTS

The distribution function should be different for contacts of small area (point contacts) and those of large area (sandwich-type junctions). We believe that for the point contacts only a few discrete realizations of LC energy are possible and may be involved in the electron tunneling. In this case $F(E)=F_{\rm pc}(E)$ is sharply peaked at these LC energies:

$$F_{\rm pc}(E)=\sum_{l=1}^{s} F_l \delta(E-E_l) \ . \tag{18}$$

The F_l's are normalization constants and s is the number of probed areas with an associated LC energy E_l. With the use of $F_{\rm pc}(E)$ we simply get

$$G_{\rm 2pc}(V,T=0)=\sum_{l=1}^{s} G_l\{\theta(-E_l)\theta(2E_l-eV) +\theta(E_l)\theta(-2E_l+eV)\} \ , \tag{19}$$

which is a spectrum of irregular steps depending on a given realization of LC level positions in the contact. If we use only one LC level position equal to its equilibrium position in the bulk CM, we will get from Eq. (16) the result obtained in Ref. 33. In sandwich-type contacts any LC energy is involved in the tunneling, and $F(E)=F_{\rm sw}(E)$ should be a smooth function of energy. The simplest model possible of the distribution function $F(E)$ is a uniform distribution:

$$F_{\rm sw}(E)=[\theta(E+\Delta)-\theta(E-\Delta)]/(2\Delta) \ , \tag{20}$$

Using this, we have from Eq. (17)

$$G_{\rm 2sw}(V,T=0)=\frac{e^2}{h}\frac{N'}{N_a N_b}N^a N^b\langle |t^c|^2|S_1-S_2|^2\rangle_{\rm average}\frac{|eV|}{2\Delta} \ . \tag{21}$$

The formulas Eq. (19) and Eq. (21) illustrate our point that the scale of the locally homogeneous regions compared to the contact area is of great importance in this model, and we suggest that this is an explanation for the difference between point-contact and sandwich-type tunneling experiments. This conclusion relies on the assumption of local pairing, which is made evident, by putting $U=0$ in Eq. (17). $|S_1-S_2|$ and G_2 will then be set to zero. The same voltage dependence within a negative-U Hubbard model was obtained in Ref. 22 without any assumption of the LC levels being disordered. This result is due to double-electron tunneling, which we consider to be less probable, and does not predict any difference between the point-contact and sandwich-type case.

We now calculate $G_{\rm 2sw}(V=0,T)$ when $k_B T \ll \Delta$, still assuming Eq. (20). Since E_1 is large we have $n_{jd}=[1+\exp(2\beta E)]^{-1}$. From Eq. (16) we get, if we scale the energies by $k_B T$,

$$\begin{aligned} I_2=&\frac{2e}{h}\frac{N'}{N_a N_b}N_F^a N_F^b\langle |t^c|^2|S_1-S_2|^2\rangle_{\rm average}\frac{(k_B T)^2}{2\Delta} \\ &\times\int_{-\beta\Delta}^{\beta\Delta} dx\int_{-\beta\varepsilon_F^{\rm CM}}^{\beta(2E-eV+\varepsilon_F^{\rm M})} dy\{n(-2k_B Tx)n(k_B Ty)n(2k_B Tx-k_B Ty-eV) \\ &-n(2k_B Tx)n(-k_B Ty)n(-2k_B Tx+k_B Ty+eV)\} \ . \end{aligned} \tag{22}$$

Since $\beta\Delta \gg 1$ and Δ is assumed to be smaller than $\varepsilon_F^{\rm M}$ and $\varepsilon_F^{\rm CM}$, the Fermi energies of the a and b band, we can extend the limits of the integral above to infinity. We then write down

$$\begin{aligned} I_2=&\frac{e}{h}\frac{N'}{N_a N_b}N_F^a N_F^b\langle |t^c|^2|S_1-S_2|^2\rangle_{\rm average}\frac{(k_B T)^2}{\Delta}\int_{-\infty}^{\infty} dx\int_{-\infty}^{\infty} dy\, n(-2k_B Tx)n(k_B Ty) \\ &\times\{n(2k_B Tx-k_B Ty-eV)-n(2k_B Tx-k_B Ty+eV)\} \ , \end{aligned} \tag{23}$$

where we have substituted $x\rightarrow -x$ and $y\rightarrow -y$ in the second term of Eq. (22). Taking the limit $V\rightarrow 0$, the difference in the integral above can be expressed as a derivative times an increment. This produces a factor $2eV/k_B T$. As a result we get

$$\begin{aligned} G_{\rm 2sw}(V=0,T)=&2\int_{-\infty}^{\infty} dx\int_{-\infty}^{\infty} dy\frac{1}{1+e^{-2x}}\frac{1}{1+e^{y}}\left[-\frac{\partial}{\partial z}\frac{1}{1+e^{z}}\right]_{z=2x-y}\frac{e^2}{h}\frac{N'}{N_a N_b}N_F^a N_F^b\langle |t^c|^2|S_1-S_2|^2\rangle_{\rm average}\frac{k_B T}{\Delta} \\ =&1.2337\frac{e^2}{h}\frac{N'}{N_a N_b}N_F^a N_F^b\langle |t^c|^2|S_1-S_2|^2\rangle_{\rm average}\frac{k_B T}{\Delta} \ . \end{aligned} \tag{24}$$

$G_{2sw}(V=0,T)$ is linear in T. This is contrary to G_0 which is not dependent on temperature. Taking the quotient

$$\gamma=\frac{G_{2sw}(V=0,T=\epsilon/k_B)}{G_{2sw}(V=\epsilon/e,T=0)}=2.4674\ , \tag{25}$$

we compare with experimental results of Ref. 4 which suggest that $\gamma_{exp}\approx 0.7$. The reason for discrepancy could be the electrode resistance, which in the case of high-T_c materials is a linear function of temperature. If this resistance is of the order 1% of the total resistance of the junction, one could obtain agreement with experiment.

Another distribution function is a Gaussian function:

$$F_{sw}(E)=\frac{1}{\sqrt{\pi}\Delta}\exp(-E^2/\Delta^2)\ . \tag{26}$$

Δ still tells the width of the distribution. Despite the smoothening, see Fig. 3, the discussion above still applies, and the value of γ is not sensitive to this different choice of distribution function.

Finally, we want to point out the asymmetry connected with the difference between the recombination process described by Fig. 2(a) and the reverse process of dissociation of a local pair. In the first case the condition $eV=2E+\varepsilon_F^{CM}$ means that all channels like (α) and (β) of Fig. 2(a) down to the band bottom of CM have been opened up by the positive bias. Further increase of voltage does not increase the current, implying zero conductance in this voltage regime. This effect is not present for dissociation of a local pair at negative bias. To illustrate the asymmetry, if we still make the approximations preceding Eq. (17), despite the larger voltage scale, we get from Eq. (16) at zero temperature

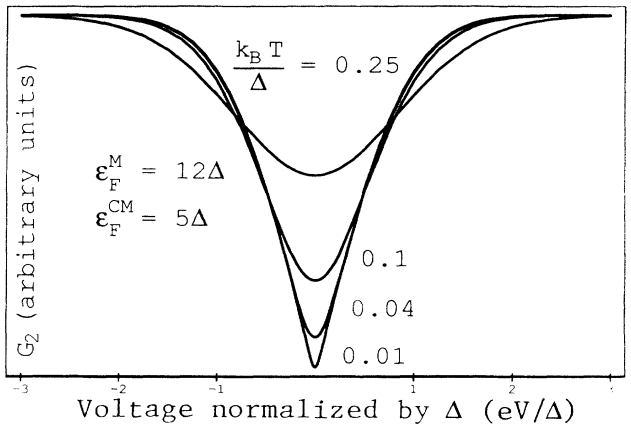

FIG. 3. G_2 as a function of voltage with $F(E)=F_{sw}(E)$ according to Eq. (26) is calculated for different temperatures.

$$\frac{dG_2}{dV}=\frac{e^3}{h}\frac{N'}{N_aN_b}N^aN^b\langle|t^c|^2|S_1-S_2|^2\rangle_{average}$$
$$\times\left\{\theta(-eV)F\left[\frac{eV}{2}\right]-\theta(eV)F\left[\frac{eV}{2}\right]+\theta(eV-\varepsilon_F^{CM})F\left[\frac{eV-\varepsilon_F^{CM}}{2}\right]\right.$$
$$\left.+\theta(eV-\varepsilon_F^{M})F\left[\frac{eV-\varepsilon_F^{M}}{2}\right]-\theta(eV-\varepsilon_F^{CM}-\varepsilon_F^{M})F\left[\frac{eV-\varepsilon_F^{CM}-\varepsilon_F^{M}}{2}\right]\right\}. \tag{27}$$

The formula above tells that we get direct information about $F(E)$, $E<0$ by taking the derivative of the conductance for $eV<0$. In the same way we derive $F(E)$, $E>0$, by examining the conductance at positive bias. In this case the information is direct only as long as the voltage is smaller than the Fermi energies of the a and b band.

Of course, there is also asymmetry connected with the fact that the local pairs could be nonsymmetrically distributed around the Fermi level.

V. CONCLUSIONS

In conclusion we propose a model of single-electron tunneling into randomly distributed local centers with strong interelectron attraction to obtain the linear temperature and voltage dependences of the tunneling conductance. Our predictions are in good agreement with existing experiments on electron tunneling in normal-state high-T_c materials.

ACKNOWLEDGMENTS

We would like to thank Z. Crljen, L. Jönsson, and J. Luberek for discussions. M. Hurd would also like to thank M. Bartkowiak for discussions. This work was supported by NFR and NUTEK.

*Also at Institute for Low Temperature Physics and Engineering, Ukr. Acad. Sci., 47 Lenin Ave., 310164 Kharkov, Ukraine.

[1]J. R. Kirtley, Int. J. Mod. Phys. B **4**, 201 (1990), review.
[2]H. Ikuta *et al.*, Jpn. J. Appl. Phys. **27**, L1038 (1988).
[3]M. Lee *et al.*, Phys. Rev. B **39**, 801 (1989).
[4]M. Gurvitch *et al.*, Phys. Rev. Lett. **63**, 1008 (1989).
[5]A. Fournel *et al.*, Europhys. Lett. **6**, 653 (1988).

[6]J. Geerk *et al.*, Physica C **162-164**, 837 (1989).
[7]I. Takeuchi *et al.*, Physica C **158**, 83 (1989).
[8]Y. Chen *et al.*, Mod. Phys. Lett. B **2**, 903 (1988).
[9]S. Zhao *et al.*, Solid State Commun. **67**, 1179 (1988).
[10]S. Vieira *et al.*, Phys. Rev. B **38**, 9295 (1988).
[11]M. R. Beasley, Nature **350**, 21 (1991).
[12]H. Tao *et al.*, Physica C **162-164**, 1127 (1989).
[13]M. D. Kirk *et al.*, Phys. Rev. B **35**, 8850 (1987).
[14]P. Chaudhari *et al.*, Phys. Rev. B **36**, 8903 (1987).
[15]J. R. Kirtley *et al.*, Phys. Rev. B **35**, 8846 (1987).
[16]R. S. Gonelli *et al.*, Phys. Rev. B **39**, 2261 (1989).
[17]P. W. Anderson and Z. Zou, Phys. Rev. Lett. **60**, 132 (1988).
[18]K. Flensberg, P. Hedegård, and M. Brix Pedersen, Phys. Rev. B **38**, 841 (1988); **40**, 850 (1989).
[19]K. Flensberg and P. Hedegård, Physica C **160**, 89 (1989).
[20]J. R. Kirtley and D. J. Scalapino, Phys. Rev. Lett. **65**, 798 (1990).
[21]J. R. Kirtley, S. Washburn, and D. J. Scalapino, Phys. Rev. B **43**, 336 (1992).
[22]Y. Bar-Yam, Phys. Rev. B **43**, 359 (1991); **43**, 2601 (1991).
[23]A. S. Alexandrov, M. P. Kazeko, and S. G. Rubin, Zh. Eksp. Teor. Fiz. **98**, 1656 (1990) [Sov. Phys. JETP **71**, 928 (1990)].
[24]H. J. van Schevicoven and A. Th. A. M. de Waele, Physica C **162-164**, 1055 (1989).
[25]M. C. Gallagher and J. C. Adler, Physica C **162-164**, 1129 (1989).
[26]I. O. Kulik, Int. J. Mod. Phys. B **1**, 851 (1988).
[27]A. S. Alexandrov, J. Ranninger, and S. Robaszkiewicz, Phys. Rev. B **33**, 4526 (1986).
[28]N. F. Mott, Adv. Phys. **39**, 55 (1990).
[29]R. I. Shekhter, G. Wendin, and I. O. Kulik, Phys. Rev. B **44**, 10 215 (1991).
[30]D. M. Newns, Phys. Rev. B **36**, 5595 (1987).
[31]P. Coleman, Phys. Rev. B **35**, 5072 (1987).
[32]J. R. Schrieffer and P. A. Wolff, Phys. Rev. **149**, 491 (1966).
[33]S. I. Beloborod'ko and I. O. Kulik, Fiz. Nizk. Temp. **15**, 787 (1989) [Sov. J. Low Temp. Phys. **15**, 435 (1989)].

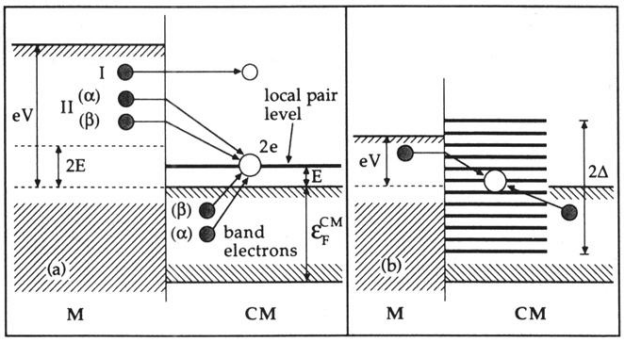

FIG. 2. (a) Diagrams of electron tunneling from the conventional metal (M) to the strongly correlated metal (CM). Process I shows tunneling from the band in M to the band in CM. Processes II (a) and (b) show different channels of tunneling from the band in M to a local center in CM accompanied by the transition from the band in CM to the same local center. $2E$ is the local pair energy relative to the chemical potential and is also the threshold energy for processes II. (b) The local pair levels are distributed in an interval of 2Δ. The case when $eV < \Delta$ is shown.